Supporting Information

$Ba_6Zn_7Ga_2S_{16}$: A Wide Band Gap Sulfide with Phase-Matchable Infrared NLO Properties

Yan-Yan Li,[1] Peng-Fei Liu,[1, 2] and Li-Ming Wu[1,*]

[1]Key Laboratory of Research on Chemistry and Physics of Optoelectronic Materials, Fujian Institute of Research on the Structure of Matter, Chinese Academy of Sciences, Fuzhou, Fujian 350002, People's Republic of China

[2]University of Chinese Academy of Sciences, Beijing 100039, People's Republic of China

E-mail: liming_wu@fjirsm.ac.cn

Table S1. Properties comparison of the known phase-matchable (PM) IR NLO chalcogenides with Eg > 3.0 eV, $AgGaS_2$ and title $Ba_6Zn_7Ga_2S_{16}$.

	Materials	Eg (eV)	LDT (×AGS)	d_{ij} (×KDP)
①	$Ba_6Zn_7Ga_2S_{16}$ (this work)	3.5	28[a]	17
②	$SnGa_4S_7$ [S1]	3.1	19[a]	43.3
③	$BaGa_4S_7$ [S2]	3.54	3[b]	33.3
④	Na_2BaSnS_4 [S3]	3.27	5[a]	10
⑤	Na_2BaGeS_4 [S4]	3.7	8[a]	17
⑥	$Na_2ZnGe_2S_6$ [S4]	3.25	6[a]	30
⑦	$LiInS_2$ [S5, S6]	3.57	2.5[b]	19
⑧	$LiGaS_2$ [S5, S7]	4.15	11[b]	15
⑨	$AgGaS_2$ [S8]	2.64	1[a]	33.3
	$BaGa_2SiS_6$ [S9]	3.75	-	33.3

[a]Measured on polycrystalline samples, [b]Measured on large single crystals.

References:

(S1) Luo, Z. Z.; Lin, C. S.; Cui, H. H.; Zhang, W. L.; Zhang, H.; He, Z. Z.; Cheng, W. D. SHG materials $SnGa_4Q_7$ (Q = S, Se) appearing with large conversion efficiencies, high damage thresholds, and wide transparencies in the mid-infrared region. *Chem. Mater*. **2014**, *26*, 2743−2749.

(S2) Lin, X. S.; Zhang, G.; Ye, N. Growth and characterization of $BaGa_4S_7$: a new crystal for mid-IR nonlinear optics. *Cryst. Growth Des.* **2009,** *9*, 1186−1189.

(S3) Li, G. M.; Wu, K.; Liu, Q. Yang, Z. H.; Pan, S. L. $Na_2ZnGe_2S_6$: a new infrared nonlinear optical material with good balance between large second-harmonic generation response and high laser damage threshold. *J. Am. Chem. Soc*. **2016**, *138*, 7422−7428.

(S4) Wu, K.; Yang, Z. H.; Pan, S. L. Na_2BaMQ_4 (M = Ge, Sn; Q = S, Se): Infrared Nonlinear Optical Materials with Excellent Performances and that Undergo Structural Transformations. *Angew. Chem. Int. Ed.* **2016**, *128*, 6825−6827.

(S5) Isaenko, L. I.; Vasilyeva, I. G.; Merkulov, A. A.; Yelisseyev, A. P.; Lobanov, S. I. Growth of new nonlinear crystals $LiMX_2$ (M = Al, In, Ga; X= S, Se, Te) for the mid-IR optics. *J. Cryst. Growth*. **2005**, *275*, 217−223.

(S6) Fossier, S.; Salaun, S.; Mangin, J.; Bidault, O.; Thenot, I.; Zondy, J. J.; Chen, W. D.; Rotermund, F.; Petrov, V.; Petrov, P.; Henningsen, J.; Yelisseyev, A.; Isaenko, L.; Lobanov, S.; Balachninaite, O.; Slekys, G.; Sirutkaitis, V. Optical, vibrational, thermal, electrical, damage, and phase-matching properties of lithium thioindate. *J. Opt. Soc. Am. B.* **2004**, *21*, 1981−2007.

(S7) Tyazhev, A.; Vedenyapin, V.; Marchev, G.; Isaenko, L.; Kolker, D.; Lobanov, S.; Petrov, V.; Yelisseyev, A.; Starikova, M.; Zondy, J. Singly-resonant optical parametric oscillation based on the wide band-gap mid-IR nonlinear optical crystal $LiGaS_2$. *J. Opt. Mater.* **2013**, 35, 1612−1615.

(S8) Harasaki, A.; Kato, K. J. New data on the nonlinear optical constant, phase-matching, and optical damage of $AgGaS_2$. *Appl. Phys*. **1997**, *36*, 700−703.

(S9) Yin, W. L.; Feng, K.; He, R.; Mei, D. J.; Lin, Z. S.; Yao, J. Y.; Wu, Y. C. $BaGa_2MQ_6$ (M= Si, Ge; Q = S, Se): a new series of promising IR nonlinear optical materials. Dalton Transactions,

2012, *41*, 5653−5661.

Table S2. Atomic coordinates and equivalent isotropic displacement parameters of $Ba_6Zn_7Ga_2S_{16}$.

Atom	Wyckoff site	*x*	*y*	*z*	U_{eq}(Å)[a]
Ba(1)	9*b*	0.35464(6)	0.08476(6)	0.24496(2)	0.0164(2)
Ba(2)	9*b*	0.43443(7)	0.40462(7)	0.11452(2)	0.0179(2)
Zn(1)	9*b*	0.3079(2)	0.4365(2)	0.31272(4)	0.0118(2)
Zn(2)	9*b*	0.0303(2)	0.2189(2)	0.04426(4)	0.0116(2)
Zn(3)	3*a*	0.0000	0.0000	0.3589(3)	0.019(2)
Zn(3')	3*a*	0.0000	0.0000	0.3350(9)	0.014(4)
Ga(1)	3*a*	0.0000	0.0000	0.53637(7)	0.0114(4)
Ga(2)	3*a*	0.0000	0.0000	0.15744(7)	0.0108(4)
S(1)	9*b*	0.4432(2)	0.1379(2)	0.01614(8)	0.0142(4)
S(2)	9*b*	0.3337(3)	0.4409(3)	0.2278(2)	0.0151(5)
S(3)	9*b*	0.2555(2)	0.1958(2)	0.34590(7)	0.0099(4)
S(4)	9*b*	0.2270(3)	0.0136(3)	0.1288(2)	0.0169(6)
S(5)	3*a*	0.0000	0.0000	0.0000(2)	0.0123(6)
S(6)	3*a*	0.0000	0.0000	0.4530(2)	0.0132(8)
S(7)	3*a*	0.0000	0.0000	0.2394(2)	0.0134(9)
S(8)	3*a*	0.0000	0.0000	0.8464(2)	0.0126(5)

[a] U(eq) is defined as one-third of the trace of the orthogonalized U_{ij} tensor.

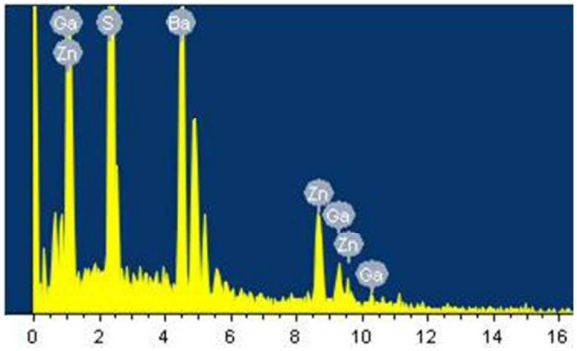

Figure S1. The EDX spectrum of $Ba_6Zn_7Ga_2S_{16}$.

Table S3. The ICP data of $Ba_6Zn_7Ga_2S_{16}$.

Comp.	Element	Weight%	Formula
$Ba_6Zn_7Ga_2S_{16}$	Ba	47.85%	$Ba_{5.9}Zn_{7.2}Ga_{2.0}$
	Zn	28.02%	
	Ga	8.25%	

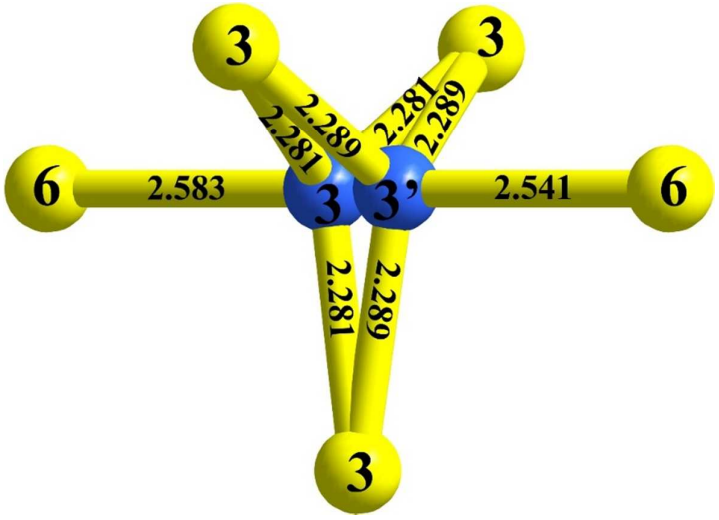

Figure S2. The coordination environments of Zn on Wyckoff site 3*e* that spliting into Zn(3) (occu.: 0.80) and Zn(3') (occu.: 0.20) with Zn−S bond length (Å) marked.

PS: The possible existing Zn(3') (occu.: 0.20) atom is very close to Zn(3), with the Zn(3)–Zn(3') distance being 0.65 Å. Additionally, the Zn(3')–S bond distances and the S–Zn(3')–S angles of the Zn(3')S_4 tetrahedron are similar to the corresponding data of the Zn(3)S_4 tetrahedron. Similar positional disorder has been found on the In atom which splits into In(2) (occu.: 0.80) and In(3) (occu.: 0.20) of compound $Ba_{12}In_4S_{19}$[S10] and the Cu atom with Cu(1) (occu.: 0.82) and Cu(2) (occu.: 0.18) of compound R_2CuInS_5 (R = La, Ce, Pr, Nd and Sm).[S11]

References:

(S10) Liu, J. W.; Wang, P.; Chen, L. Contribution of disulfide S_2^{2-} anions to the crystal and electronic structures in ternary sulfides, $Ba_{12}In_4S_{19}$, $Ba_4M_2S_8$ (M= Ga, In). *Inorg. Chem*. **2011**, *50*, 5706–5713.

(S11) Jin, G. B.; Choi, E. S.; Guertin, R. P.; Booth, C. H.; Albrecht-Schmitt, T. E. Syntheses, structure, magnetism, and optical properties of the ordered interlanthanide copper chalcogenides Ln_2YbCuQ_5 (Ln= La, Ce, Pr, Nd, Sm; Q= S, Se): evidence for unusual magnetic ordering in Sm_2YbCuS_5. *Chem. Mater*. **2011**, *23*, 1306–1314.

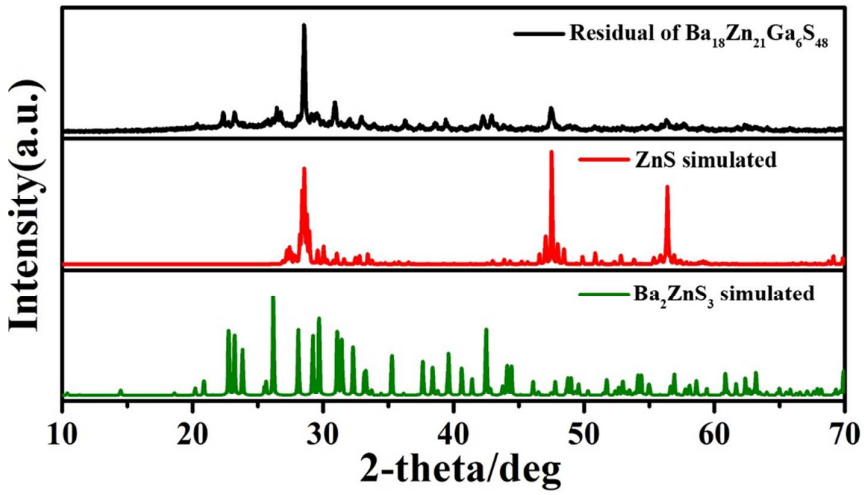

Figure S3. Powder X-ray diffraction patterns of samples obtained after TG and DTA measurements of $Ba_6Zn_7Ga_2S_{16}$, indicating that this compound was mainly decomposed into ZnS and Ba_2ZnS_3.

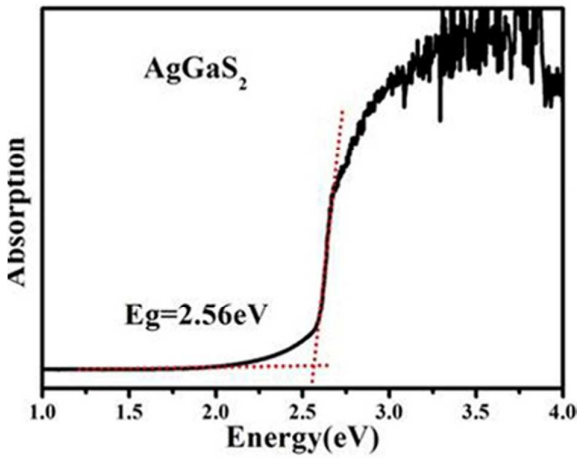

Figure S4. Diffuse reflection spectra of $AgGaS_2$.

Table S4. Selected bond lengths (Å) of $Ba_6Zn_7Ga_2S_{16}$.

Bond	dist.	bond	dist.
Ba(1)–S(1)	3.422(2)	Zn(2)–S(1)	2.319(2)
Ba(1)–S(2)	3.387(2)	Zn(2)–S(3)	2.335(2)
Ba(1)–S(2)	3.591(2)	Zn(2)–S(4)	2.319(3)
Ba(1)–S(2)	3.617(3)	Zn(2)–S(5)	2.337(2)
Ba(1)–S(3)	3.255(2)	Zn(3)–Zn(3')	0.65(2)
Ba(1)–S(4)	3.319(3)	Zn(3)–S(3)	2.290(2)
Ba(1)–S(5)	3.672(2)	Zn(3)–S(3)	2.290(2)
Ba(1)–S(7)	3.1383(6)	Zn(3)–S(3)	2.290(2)
Ba(1)–S(8)	3.301(3)	Zn(3)–S(6)	2.54(2)
Ba(2)–S(1)	3.458(2)	Zn(3')–S(3)	2.281(4)
Ba(2)–S(2)	3.285(3)	Zn(3')–S(3)	2.281(4)
Ba(2)–S(3)	3.187(2)	Zn(3')–S(3)	2.281(4)
Ba(2)–S(4)	3.333(3)	Zn(3')–S(7)	2.58(3)
Ba(2)–S(4)	3.544(3)	Ga(1)–S(2)	2.307(3)
Ba(2)–S(6)	3.1753(6)	Ga(1)–S(2)	2.307(3)
Ba(2)–S(8)	3.212(3)	Ga(1)–S(2)	2.307(3)
Zn(1)–S(1)	2.298(2)	Ga(1)–S(6)	2.252(5)
Zn(1)–S(1)	2.346(2)	Ga(2)–S(4)	2.289(3)
Zn(1)–S(2)	2.307(3)	Ga(2)–S(4)	2.289(3)
Zn(1)–S(3)	2.323(2)	Ga(2)–S(4)	2.289(3)
		Ga(2)–S(7)	2.213(5)

Table S5. Selected angles (deg) of $Ba_6Zn_7Ga_2S_{16}$.

bond	angle	bond	angle
S(1)–Zn(1)–S(2)	111.53(9)	S(3)–Zn(3')–S(3)	118.4(3)
S(1)–Zn(1)–S(3)	109.90(7)	S(3)–Zn(3')–S(3)	118.4(3)
S(2)–Zn(1)–S(3)	111.66(9)	S(3)–Zn(3')–S(3)	118.4(3)
S(1)–Zn(1)–S(1)	100.5(2)	S(3)–Zn(3')–S(7)	97.4(6)
S(2)–Zn(1)–S(1)	120.59(9)	S(3)–Zn(3')–S(7)	97.4(6)
S(3)–Zn(1)–S(1)	101.73(7)	S(3)–Zn(3')–S(7)	97.4(6)
S(1)–Zn(2)–S(4)	100.05(9)	S(6)–Ga(1)–S(2)	106.81(8)
S(1)–Zn(2)–S(3)	102.09(8)	S(6)–Ga(1)–S(2)	106.81(8)
S(4)–Zn(2)–S(3)	118.81(9)	S(2)–Ga(1)–S(2)	111.99(7)
S(1)–Zn(2)–S(5)	112.16(8)	S(6)–Ga(1)–S(2)	106.81(8)
S(4)–Zn(2)–S(5)	123.0(2)	S(2)–Ga(1)–S(2)	111.99(7)
S(3)–Zn(2)–S(5)	99.24(7)	S(2)–Ga(1)–S(2)	111.99(7)
S(3)–Zn(3)–S(3)	117.7(2)	S(7)–Ga(2)–S(4)	109.74(7)
S(3)–Zn(3)–S(3)	117.7(2)	S(7)–Ga(2)–S(4)	109.74(7)
S(3)–Zn(3)–S(3)	117.7(2)	S(4)–Ga(2)–S(4)	109.20(8)
S(3)–Zn(3)–S(6)	98.8(2)	S(7)–Ga(2)–S(4)	109.74(7)
S(3)–Zn(3)–S(6)	98.8(2)	S(4)–Ga(2)–S(4)	109.20(8)
S(3)–Zn(3)–S(6)	98.8(2)	S(4)–Ga(2)–S(4)	109.20(8)

Table S6. The direction and magnitude (Debye: D) of dipole moments of the building units in $Ba_6Zn_7Ga_2S_{16}$.

Building unit	**X**	**Y**	**Z**	Symmetry operation
$Zn(3)S_4$	**0**	**0**	**0.65**	
1^{st} $Zn(1)S_4$	0.62	0.31	1.26	(X,Y,Z)
2^{nd} $Zn(1)S_4$	-0.31	0.31	1.26	(-Y,X-Y,Z)
3^{rd} $Zn(1)S_4$	-0.31	-0.62	1.26	(-X+Y,-X,Z)
$Ga(1)S_4$	0	0	-1.98	
$Zn(1)_3Ga(1)S_{10}$	**0**	**0**	**1.80**	
1^{st} $Zn(2)S_4$	-1.43	-1.61	-1.13	(X,Y,Z)
2^{nd} $Zn(2)S_4$	1.61	0.18	-1.13	(-Y,X-Y,Z)
3^{rd} $Zn(2)S_4$	-0.18	1.43	-1.13	(-X+Y,-X,Z)
$Ga(2)S_4$	0	0	1.37	
$Zn(2)_3Ga(2)S_{10}$	**0**	**0**	**-2.02**	
A basic repeating unit of $[Zn(1)_3Zn(2)_3Zn(3)Ga(1)Ga(2)S_{22}]$	**0**	**0**	**0.43**	

Table S7. The results of polycrystalline LDTs for $Ba_6Zn_7Ga_2S_{16}$ and $AgGaS_2$ in the same particle size range of 150−210 μm.

Comp.	Damage energy (mJ)	Spot area (cm^2)	Damage threshold (MW/cm^2)
$Ba_6Zn_7Ga_2S_{16}$	28.61	0.0707	40.47
$AgGaS_2$	4.21	0.292	1.44

Table S8. The calculated total energies of model-0, model-1 and model-2 of $Ba_6Zn_7Ga_2S_{16}$, in which Zn(3) atom (Zn(1) and Zn(2): Wyckoff site 9*b*) taking any one of all three 3*a* Wyckoff sites (Zn(3), Ga(1) and Ga(2): Wyckoff site 3*a*) in the tetrahedral centre.

Comp.	model	Total energy (eV)
$Ba_6Zn_7Ga_2S_{16}$	0	0
	1	0.67
	2	1.17